Terbit *online* pada laman web jurnal : http://metal.ft.unand.ac.id

METAL: Jurnal Sistem Mekanik dan Termal

| ISSN (Print) 2598-1137 | ISSN (Online) 2597-4483 |

Research article

Experimental and Computational Analysis of UHMWPE-Based Multi-Layered Bulletproof Vests Under 9mm Projectiles Impact

Hizkia Timotius, Azhari Sastranegara[*]*, Rendi Hernawan, Nanang Ali Sutisna, Lydia Anggraini*

Department of Mechanical Engineering, President University, Indonesia

ARTICLE INFORMATION

Article History:
Received : 10 January 2025
Revised : 17 April 2025
Accepted : 30 April 2025

KEYWORDS

Ballistic Impact
Bulletproof Vest
FEM Simulation
UHMWPE

CORRESPONDENCE

E-mail: azhari.sastranegara@president.ac.id

A B S T R A C T

This study investigates the ballistic performance and energy absorption of multi-layered UHMWPE bulletproof vests against 9mm projectiles using experiments and finite element simulations (LS-DYNA). Two configurations were analyzed: a conventional structure and a sandwich-layered design incorporating UHMWPE, titanium (Ti6Al4V), and PVC. Ballistic tests, conducted per NIJ Level IIIA standards, were validated through simulations. The sandwich-layered vest exhibited superior energy dissipation, achieving BFS values of 12.03 mm (experiment) and 12.36 mm (simulation), effectively reducing blunt trauma risk. The multi-material approach enhanced penetration resistance and impact force distribution, while numerical models closely matched experimental findings, confirming reliability. Results demonstrate the feasibility of lightweight, high-performance ballistic armor. Future work will explore material optimization, configuration refinements, and testing with higher-caliber projectiles for broader applications.

1. INTRODUCTION

The increasing demands of modern warfare and law enforcement have emphasized the importance of lightweight yet highly efficient body armor capable of providing superior protection [1], [2]. Among the various materials explored, Ultra-High Molecular Weight Polyethylene (UHMWPE) has emerged as a promising candidate due to its remarkable impact resistance, high tensile strength, and low density [3], [4]. These properties make UHMWPE an ideal core material for ballistic applications. However, the challenge remains to design bulletproof vests that can achieve optimal performance against high-velocity impacts while maintaining flexibility, durability, and wearer comfort [5] .

Conventional body armor designs often struggle to balance lightweight construction with sufficient protection against multi-impact scenarios or higher-caliber projectiles [6]. While UHMWPE demonstrates impressive energy absorption capabilities, studies have indicated that its standalone performance can be insufficient in mitigating blunt trauma or resisting sustained impacts from high-velocity projectiles [7]–[9]. Research has shown that incorporating rigid reinforcements, such as ceramic or titanium layers, can enhance penetration resistance; however, such configurations often introduce significant weight and compromise user mobility [10]–[12]. Additionally, the integration of polymeric layers, such as polyvinyl chloride (PVC), has shown potential in reducing backface deformation and absorbing shock, but these approaches remain underexplored in conjunction with UHMWPE and rigid materials [13], [14].

To address these limitations, this study proposes a novel multi-layered bulletproof vest design that combines UHMWPE, titanium (Ti6Al4V), and PVC layers in a sandwich structure. UHMWPE

https://doi.org/ 10.25077/metal.9.1.1-13.2025

serves as the primary energy-absorbing material, titanium enhances resistance to penetration, and PVC mitigates blunt trauma by distributing impact forces. This configuration aims to optimize ballistic performance while maintaining lightweight properties and wearer comfort. The ballistic performance of these designs is assessed through experimental testing in accordance with NIJ Standard-0101.04, using 9mm full metal jacket (FMJ) projectiles. Additionally, finite element simulations conducted using LS-DYNA software validate the experimental findings and provide deeper insights into the behavior of multi-layered vests under ballistic impacts [6], [15], [16].

The primary objectives of this study are: (1) to analyze the ballistic impact behavior of UHMWPE-based multi-layered vests, and (2) to identify the optimal configuration for energy absorption. By integrating experimental results with numerical simulations, this study contributes to the broader understanding of how multi-material configurations can enhance ballistic performance. These findings provide a practical framework for advancing protective gear design, bridging the gap between material science and real-world applications.

2. PROBLEM DESCRIPTION

The demand for lightweight yet highly effective ballistic protection continues to grow, especially for law enforcement and military applications. Ultra-High Molecular Weight Polyethylene (UHMWPE) has emerged as a strong candidate due to its excellent energy absorption and impact resistance. However, a major challenge remains—balancing protection, weight, and flexibility. While UHMWPE can effectively stop bullets, it struggles with mitigating blunt force trauma (backface signature, BFS) and resisting high-velocity impacts, particularly in multi-hit scenarios.

One common approach to improving ballistic performance is layering UHMWPE with additional materials, such as ceramics or metals. While these reinforcements enhance penetration resistance, they often add significant weight, making the vest less comfortable and restricting mobility. This trade-off between protection and practicality is a key issue that needs to be addressed.

To tackle this, this study explores two different vest configurations: one with a simpler structure and another with a sandwich-layered design incorporating UHMWPE, titanium (Ti6Al4V), and PVC. The goal is to find an optimal balance—enhancing protection while keeping the vest as lightweight and flexible as possible. By combining experimental testing and finite element simulations, this research aims to provide deeper insights into how different material combinations affect ballistic performance and wearer safety.

3. METHOD

The methodology of this study is divided into five main stages: material selection, experimental testing, and numerical simulation, followed by a comprehensive data analysis to compare results and derive design recommendations. Fig.1 shows the flowchart of research in this study. The primary materials used in this research are UHMWPE, Titanium Ti6Al4V, and PVC. UHMWPE serves as the core material due to its excellent tensile strength and energy absorption properties, while titanium enhances penetration resistance, and PVC functions as a shock-absorbing layer to reduce blunt trauma. These materials were arranged in two vest configurations: a simpler configuration with fewer layers and a more advanced sandwich-layered design to evaluate performance variations [1], [17]–[19].

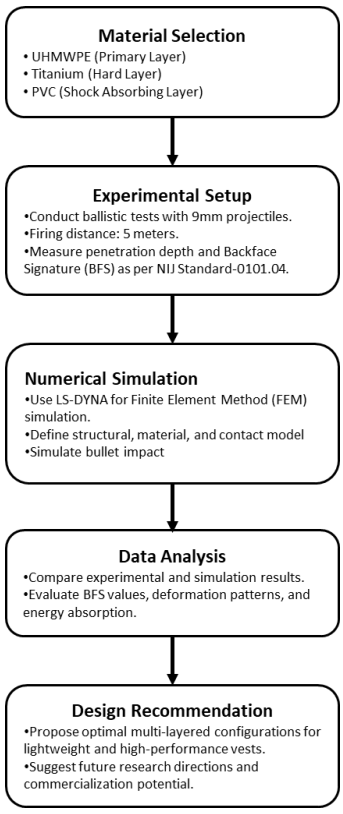

Figure 1. Methodology Flowchart

 https://doi.org/ 10.25077/metal.9.1.1-13.2025

3.1. Material Selection

The primary material used in this study is Ultra-High Molecular Weight Polyethylene (UHMWPE), a durable polymer with high tensile strength and strong impact resistance [1], [20]. UHMWPE fibers were acquired in yarn form, with material properties provided by Astra Otoparts Laboratory in Bekasi. The design also incorporates Titanium Ti6Al4V as a hard layer for improved penetration resistance and Polyvinyl Chloride (PVC) as a shock-absorbing layer [13], [23].

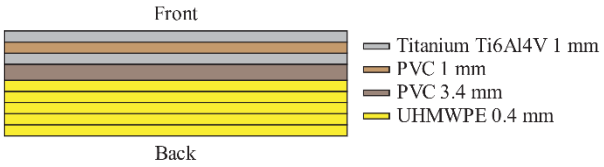

Figure 2. Structure of Vest 1

Table 1. Structure of Vest 1

Material	Qty	Thickness (mm)	Weight (gr)
UHMWPE	5	0.4	829
PVC	1	3.4	
PVC	1	1	
Titanium	1	1	

These materials were arranged in two vest configurations:

- Vest 1

Vest 1 is a handmade multi-layered vest with a thickness of 7.4 mm. This configuration comprises 5 layers of UHMWPE (Ultra-High Molecular Weight Polyethylene), 2 layers of PVC (Polyvinyl Chloride), and 1 layer of Titanium. The layers are arranged to balance weight and ballistic resistance, following a layout designed for energy absorption and impact dispersion. Each UHMWPE layer is 0.4 mm thick, while the Titanium layer provides additional hardness to resist penetration. The total weight of Vest 1 is approximately 829 grams. Fig.2 displays the layer arrangement of the specimen, while Table 1 presents detailed dimensions and layer thicknesses of the structure.

- Vest 2

Vest 2 is a multi-layered vest with a thickness of 12.7 mm, designed in a sandwich structure. It includes 10 layers of UHMWPE, 2 layers of Titanium, and 2 layers of PVC. This structure was specifically designed to enhance ballistic resistance through layered reinforcement. The UHMWPE layers are each 0.4 mm thick, while the Titanium layers add durability and resistance to the vest. The complete weight of Vest 2 is 1164 grams. The specific layer arrangement is illustrated in Fig.3, with Table 2 detailing the dimensions and layer measurements. Fig.4 provides the numerical model representation of Vest 2, demonstrating the structured arrangement used in simulations.

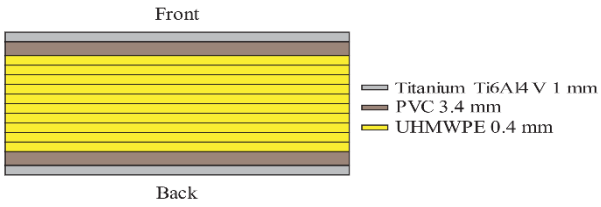

Figure 3. Structure of Vest 2

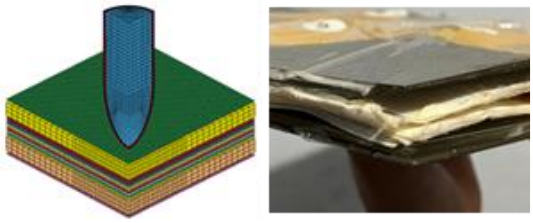

Figure 4 Vest 2 – Numerical Models and Prototypes

Table 2. Structure of Vest 2

Material	Qty	Thickness (mm)	Weight (gr)
Titanium 1	1	1	
PVC 1	1	3.4	
UHMWPE	10	0.4	1164
PVC 2	1	3.4	
Titanium 2	1	1	

These vest designs were used in experimental and numerical analyses to evaluate ballistic performance under impact from 9 mm projectiles. The goal was to assess and compare how each configuration absorbs impact energy and minimizes backface deformation, helping to identify optimal layering for commercial applications.

3.2. Experimental Test

The ballistic performance of the multi-layered UHMWPE-based vests was evaluated using controlled ballistic testing according to NIJ Standard-0101.04. The experiment involved firing 9x19 mm Full Metal Jacket (FMJ) projectiles at a series of test specimens from an STZA 12 mobile firing test platform. This platform was positioned to launch bullets at an initial speed of 380 m/s with accuracy, and shots were fired at a range of 5 meters from the vest, at angles of both 0 degrees (perpendicular) and 30 degrees [15]. The aim was to replicate conditions that law enforcement or military personnel might encounter. The firing test layout is described in Fig.5. The bullet illustration is shown in Fig.6. It is a full metal jacket with a round-nose bullet. Its materials are Brass 72 (CuZn28) for the jacket and Lead Antimony for the core metal. Details for the firing weapon and the bullets are shown in Table 3.

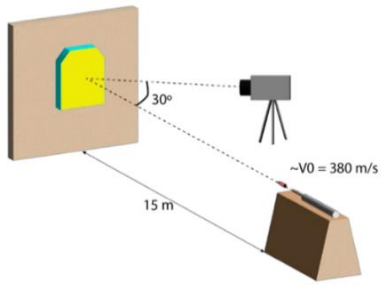

Figure 5. Illustration of experimental test setup

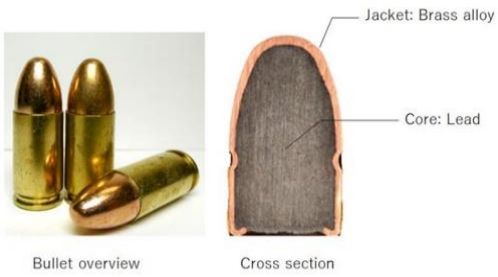

Figure 6. The Pindad MU-1TJ 9mm: A Cross-Sectional View

The bullets' penetration depth widely known as backface signature (BFS) were recorded using clay layer put at the back of the vest. The BFS values help evaluate the extent of blunt force trauma the wearer might experience, with NIJ standards requiring BFS to stay under 44 mm to prevent serious injury [15].

Table 3. Weapon Information

Specification	Details
Weapon Used	STZA 12 mobile firing test
Bullet Type	Pindad MU-1TJ 9x19 mm FMJ
Velocity	380 m/s
Bullet Mass	12.26 grams
Shoot Distance	15 meters
Bullet Material	Brass 72 (CuZn28) jacket, Lead Antimony core
Ammunition Length	29.70 mm
Average Gas Pressure	Max. 2600 kg/cm²
Accuracy at 25 meters	Max. Ø 14 cm

3.3. Numerical Simulation

To complement the experimental testing, Finite Element Method (FEM) simulations were conducted using LS-Dyna®, applying the explicit method approach, a commonly used technique for analyzing nonlinear and significant deformation events like high-velocity impacts. These simulations were essential for modeling complex material interactions under high-speed impact without the constraints of physical testing limitations [8].

The details of the model and the material properties used in this research are explained below.

- Vests Model and The Mesh Size: The model represented a quarter of the full vest model to reduce computational cost. UHMWPE layers are modeled in shell elements, while Titanium layer, PVC layer, and the bullet are modeled in hexahedral solid elements. The mesh was set to the finest size allowed by the personal computer used in this work. Accurate meshing was critical for capturing high-stress regions (like bullet entry points) and ensuring reliable simulation results. The refined element sizes are applied in high-deformation areas, to enable accurate assessment of deformation and penetration patterns [24], [25].
- Material Properties:
  - UHMWPE

 https://doi.org/ 10.25077/metal.9.1.1-13.2025

The model used for the UHMWPE layer is MAT_FABRIC. As shown in Table 4, UHMWPE properties include a density of 9.700e-09 Ton/mm^3, Young's modulus of 700 MPa, and Poisson's ratio of 0.33, with a maximum strain limit of 0.5%. The ADD_EROSION keyword was used to simulate material damage [21], [22].

Table 4. Mechanical properties of the UHMWPE layer for ADD_EROSION and MAT_FABRIC material models

Property	Value	Unit
Density, ρ	9.70e-09	Ton / mm^3
Young Modulus Longitudinal, EA	700	MPa
Young Modulus Transverse, EB	700	MPa
Minor Poisson Ratio, υBA	0.33	-
Major Poisson Ratio, υAB	0.33	-
Shear Modulus, GAB	180	MPa
Rayleigh Damping, DAMP	0.1	%
Maximum Strain, εf	0.5	%

- TitaniumTi6Al4V

The material model for the titanium alloy is MAT_PIECEWISE_LINEAR_PLASTICITY. Titanium properties shown in Table 5, include a density of 4.430e-08 Ton/mm^3, Young's modulus of 114 GPa, yield stress of 140 MPa, and strain rate sensitivity, using the Cowper-Symonds model to capture its response under impact [21], [22].

Table 5. Mechanical Properties of Titanium Ti6Al4V for MAT_PIECEWISE_LINEAR_PLASTICITY material model

Property	Value	Unit
Density, ρ	4.430e-08	Ton / mm^3
Young Modulus, E	1.140e+05	MPa
Poisson Ratio, υ	0.34	-
Yield Stress, SY	140	MPA
Tangent Modulus, ETAN	1.25	MPa
Failure Flag	0.54	-
Strain Rate Parameter, c	10	-

- PVC

The material model for the PVC layer is MAT_PLASTICITY_POLYMER. With properties shown in Table 6, PVC has a density of 1.100e-09 Ton/mm^3, Young's modulus of 10 GPa, and Poisson's ratio of 0.38. The polymer's stress-strain behavior is modeled for true strain, capturing its plastic and elastic properties under load [21], [22].

Table 6. Mechanical Properties of Polymer for MAT_PLASTICITY_POLYMER material model

Property	Value	Unit
Density	1.100e-09	Ton / mm^3
Young Modulus	1.000e+04	MPa
Poisson Ratio	0.38	-

- Bullet

The bullet's material model is MAT_JOHNSON_COOK with properties shown in Table 7. This material model is chosed to incorporate the effect of thermal effects on the structure deformation [21], [22].

Table 7. Mechanical Properties of the bullet for MAT_JOHNSON_COOK material model

Property	Lead	Brass	Unit
A	1	111.69	Mpa
B	55.551	504.69	Mpa
N	0.098	0.42	-
C	0.230	0.009	-
M	1	1.68	-
D1	-	0	-
D2	-	2.65	-
D3	-	-(0.62)	-
D4	-	0.028	-
D5	-	0	-
Tm	760	988	K
Tr	293	293	K
ε0	5.000e+04	5.000e+04	s^-1
Cp	1.240e+10	3.850e+10	N.mm/Ton.K

The above setup's primary objective was to generate accurate results with reduced computational time using symmetry and optimized meshing. This approach provides a reliable foundation for analyzing vest performance under actual impact scenarios by representing the essential physics of ballistic impacts and carefully chosen material models.

Table 8. Summary of Model Parts, Element, and Material model

Part Name	Element Model	Material Model
Vest 1 & 2 - Titanium	Shell	MAT_PIECEWISE_LINEAR_PLASTICITY
Vest 1 & 2 – Polymer	Solid	MAT_PLASTICITY_POLYMER
Vest 1 & 2 – UHMWPE	Shell	MAT_FABRIC
Bullet Jacket Model – Lead	Solid	MAT_JOHNSON_COOK
Bullet Jacket Model – Brass	Solid	MAT_JOHNSON_COOK

The summary of element types and material models of each part is shown in Table 10. The contact between bullet and vest, and the contact within each layer is modelled using contact algorithm of CONTACT_ERODING_SURFACE_TO_SURFACE. This contact allows deleting failure elements that no longer have physical influence in the simulation.

3.4. Experimental Results

The ballistic performance of two vest configurations, Vest 1 and Vest 2, was evaluated experimentally under controlled conditions. Key metrics included Backface Signature (BFS), structural deformation, and the ability to withstand multiple impacts. The deformed vests after ballistics tests are shown in Table 9. The detailed results for each vest are discussed below.

Table 9. Final Deformation Condition

Specimen	**Vest 1**	**Vest 2**
Front Face Condition		
Back Face Condition		

- **Vest 1**: The straightforward configuration, consisting of 5 layers of UHMWPE, 2 layers of PVC, and 1 titanium layer, exhibited significant structural deformation with BFS values ranging from 31.13 mm to 38.03 mm for not-fully-penetrated cases. Even though it is within the standard limit of 44 mm from the National Institute of Justice (NIJ) Level IIIA, indicating suboptimal performance in reducing blunt trauma. Moreover, the vest was fully penetrated 2 times from 6 ballistics tests, demonstrating its limited energy absorption capacity and inability to perfectly prevent full penetration.
- **Vest 2**: The sandwich-layered configuration, comprising 10 layers of UHMWPE, 2 layers of PVC, and 2 titanium layers, outperformed Vest 1 in all metrics. BFS values ranged from 9.88 mm to 16.36 mm, significantly below the NIJ standard limit, reflecting superior energy dissipation and reduced risk of blunt trauma. Unlike Vest 1, Vest 2 successfully withstood six consecutive ballistics tests without compromising structural integrity. The inclusion of additional UHMWPE layers and a balanced multi-material design enabled more efficient distribution of kinetic energy and minimized backface deformation.

3.5. Numerical Simulation Results

FEM simulations using LS-DYNA explicit code are used to validate the above experimental findings and provide insights into the dynamic behavior of the multi-layered vests under ballistic impact.

The deformation history of Vest 1 and Vest 2 is shown in Table 10. It shows that the bullet fully penetrated the Vest 1, contrarily the bullet was stopped by the Vest 2. These results align with the experimental output.

Table 10. Deformation History of Vest 1 (left) and Vest 2 (right)

Vest 1 (Time step)	**Vest 2 (Time step)**
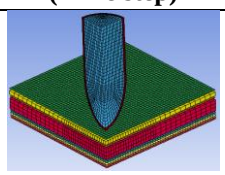	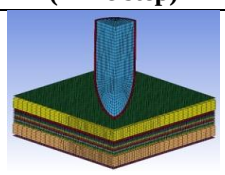
Time = 0 s	Time = 0 s

 https://doi.org/ 10.25077/metal.9.1.1-13.2025

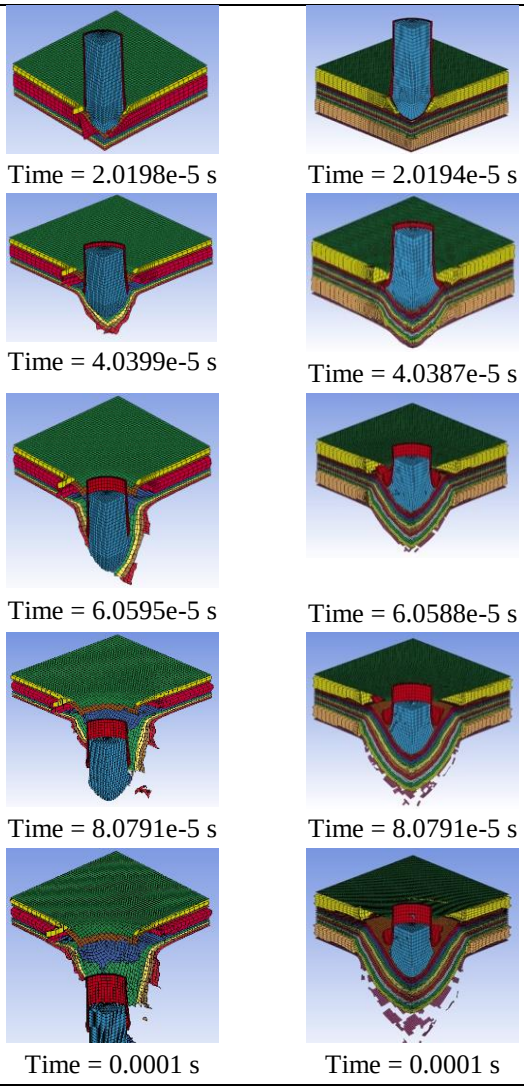

The simulation results are numerically validated by the small portion of the artificial energy generated and the conservation of energy throughout the simulation. The artificial energy generated was sliding energy and hourglass energy. These values should be lower than 10%. The conservation energy was judged from the energy ratio that should be near to 1 as widely accepted [21], [22], [24], [25]. The results in Fig.7 – Fig.10 show that the simulation had minimum numerical errors and numerically stable.

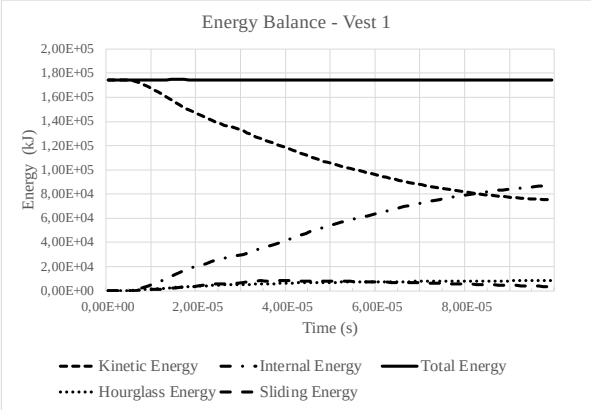

Figure 7. Vest 1 – Energy Balance

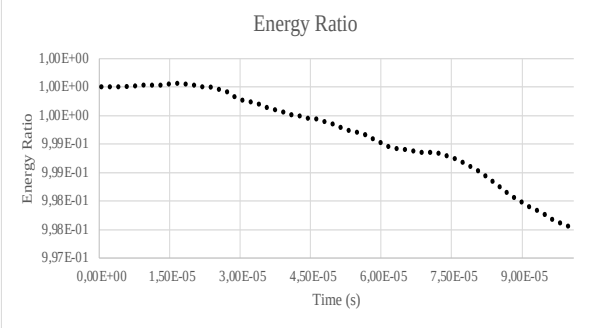

Figure 8. Vest 1 – Energy Ratio

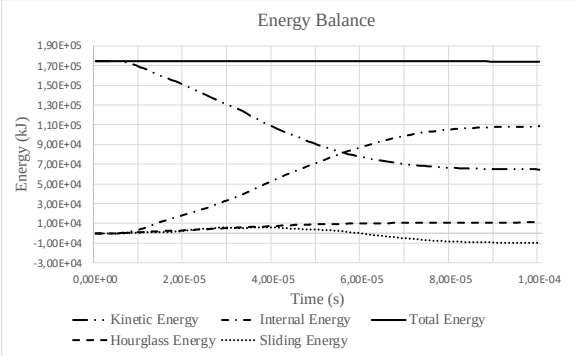

Figure 9. Vest 2 – Energy Balance

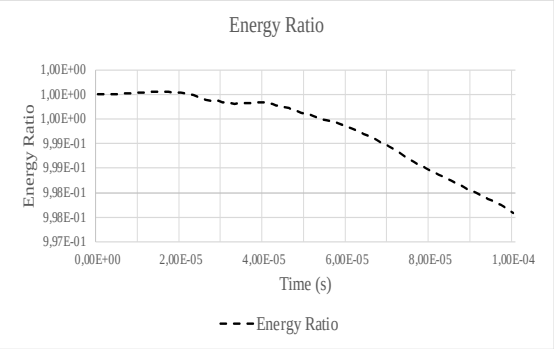

Figure 3. Vest 2 – Energy Ratio

The next step is comparing the experimental and the simulation results which are presented consecutively for each vest as follows.

- **Vest 1**
  Deformation comparison of experimental and simulation results is shown in Table 11. The bullet fully penetrated all layers in both cases. Unfortunately, the deformed bullet could be found after the experiment thus could not be compared to the simulation result.

Table 11. Comparison of Experimental and Simulation Results for Vest 1

Layer No.	Experimental Result	Simulation Result
1	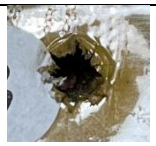	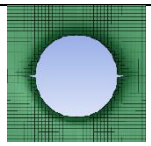
2		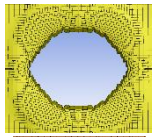
3		
4		
5		
6		
7		
Bullet	No Bullet Found	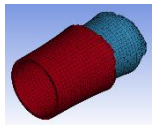

The kinetic energy history in Fig.11 shows a significant decay throughout the simulation. However, the bullet did not stop until the end of simulation. This is consistent with evidence that the bullet penetrated all layers

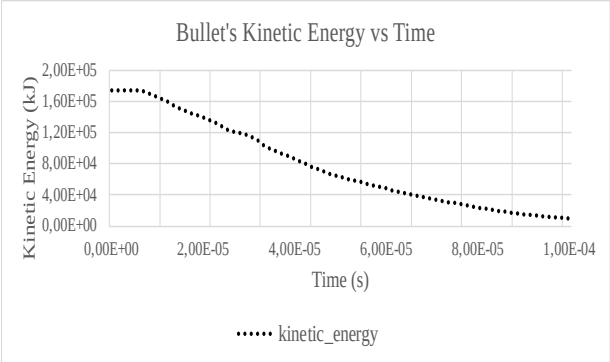

Figure 11. Vest 1 – Bullet's Kinetic Energy

- **Vest 2**
  Deformation comparison of experimental and simulation results is shown in Table 13. Clearly the bullet was stopped within the vest in experiment, and the simulation result showed the same. The deformed bullet shows excellent similarity between experiment and simulation result. However, the spalling phenomenon observed in the simulation indicated by the failure of layer 6 and 7. On the other hand, this phenomenon was not clearly observed in the experiment.

Table 12. Comparison of Experimental and Simulation Results for Vest 2

Layer No.	Experimental Result	Simulation Result
1		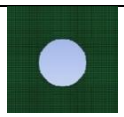
2	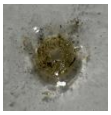	
3		
4		
5	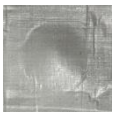	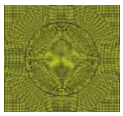

 https://doi.org/ 10.25077/metal.9.1.1-13.2025

6		
7		
Bullet		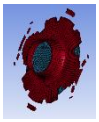

The kinetic energy history in Fig.12 shows a more drastic decay throughout the simulation. However, the bullet did not stop until the end of simulation. This is consistent with evidence that the bullet penetrated all layers.

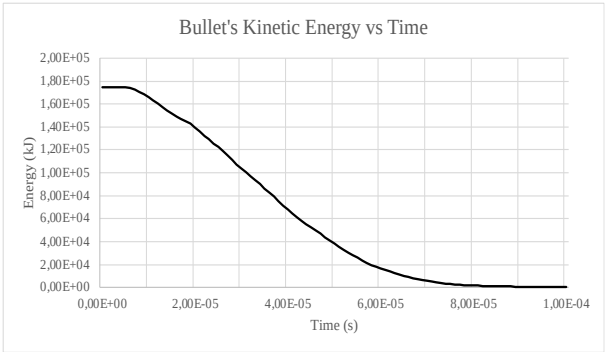

Figure 4. Vest 2 – Bullet's Kinetic Energy

The comparison of BFS in Table 13 shows that for Vest 1, the bullet fully penetrates all layers thus there is no BFS value that exists. On the other hand, the experimental results show 3 cases of fully penetrated case and 3 cases of unpenetrated one. The minimum BFS value for unpenetrated cases is 31.13 mm. Both simulation and experiment results are consistent in showing large deformation and insufficient protection against the bullet.

Still from the same table, for Vest 2, the BFS value shown in experimental results ranges from 9.90 mm to 12.03 mm. This phenomenon agrees well with the simulation result that shows 12.36 mm for the BFS value.

Table 13. Comparative Analysis of BFS (All Vest)

Vest	Simulation Result BFS	Experiment Result BFS
Vest 1	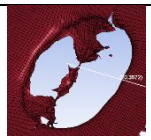 fully penetrated	Min: 31.13 mm Max: fully penetrated
Vest 2	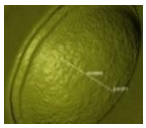 12.36 mm	Min: 9.90mm Max: 12.03 mm

3.6. Comparative Analysis

The performance of Vest 1 and Vest 2 was evaluated across key metrics, including BFS, energy absorption, and resistance to multiple impacts.

1. **Backface Signature (BFS)**: Vest 2 achieved BFS values well within NIJ standards, outperforming Vest 1 by a significant margin. The reduced BFS indicates a lower risk of blunt trauma for the wearer, making Vest 2 a more viable option for practical applications.
2. **Energy Dissipation**: Numerical simulations revealed that Vest 2 absorbed and distributed kinetic energy more efficiently than Vest 1. As shown in energy balance analyses, the additional UHMWPE layers in Vest 2 contributed to a rapid reduction in bullet kinetic energy.
3. **Structural Integrity**: While Vest 1 allowed 3 fully penetrated cases out of 6 tests, Vest 2 maintained its capability to totally stop the bullet for six consecutive tests, validating the effectiveness of its layered configuration.

3.7. Proposed Design

Based on the findings from Vest 1 and Vest 2, two new designs—Vest 3 and Vest 4—were proposed, both incorporating UHMWPE, Titanium, and PVC to optimize ballistic protection:

- Vest 3 (Sandwich Structure): Composed of 20 UHMWPE layers sandwiched between PVC layers, with Titanium plates on the front and back. This design is expected to minimize deformation and penetration effectively. The structure of Vest 3 is shown in Fig.13.

- Vest 4 (Double Front Face Structure): Features a double Titanium front with a PVC layer in between and 20 UHMWPE layers at the back. This structure enhances frontal impact resistance, making it lightweight, flexible, and capable of withstanding multiple high-velocity impacts. The structure of Vest 4 is shown in Fig.14.

Simulation Results:

- The deformation history of Vest 3 and Vest 4 is shown in Fig.15. Both vests successfully stop the bullet. Vest 3 stop the bullet faster and the penetration distance is smaller than that of Vest 4.
- Vest 3 shows a rapid initial decrease in bullet kinetic energy; thus, it has excellent energy absorption capability. However, it is only slightly better than Vest 2. This indicates that the effect of additional UHMPE layers was not very significant. There is indication that spalling phenomenon occurs in Vest 3 which add risk to the wearer.
- Vest 4 absorbs energy more gradually but eventually stops the bullet. It shows significantly better performance than Vest 1. The additional UHMWPE layers show considerable effect. The kinetic energy reduction capability of Vest 4 equals Vest 3 and Vest 2.

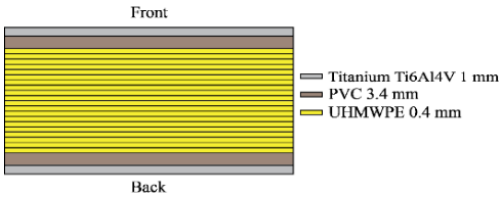

Figure 13. Structure of Proposed Design Vest 3

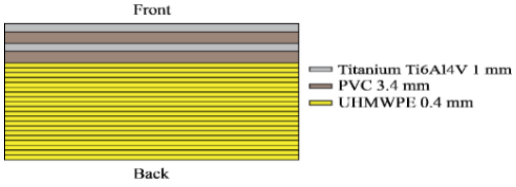

Figure 14. Structure of Proposed Design Vest 4

Table 14. Deformation History of Proposed Design Vest 3 and Vest 4

Vest 3 (Time step)	Vest 4 (Time step)
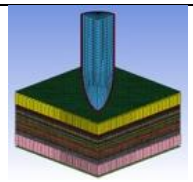 0 s	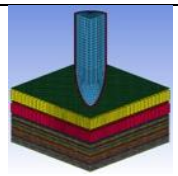 0s
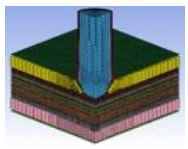 2.0194e-5 s	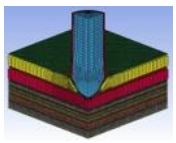 2.0194e-5 s
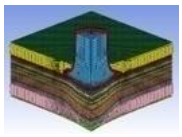 4.0392e-5 s	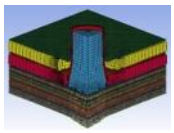 4.0392e-5 s
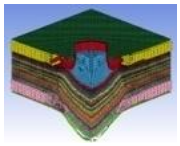 6.06e-5 s	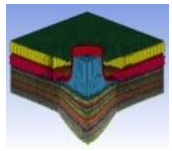 6.06e-5 s
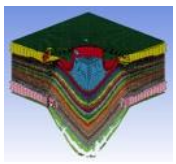 8.0797e-5 s	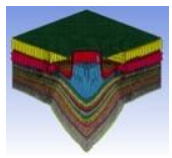 8.0797e-5 s
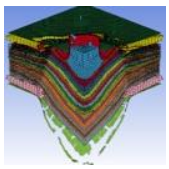 0.0001 s	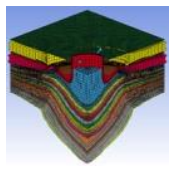 0.0001 s

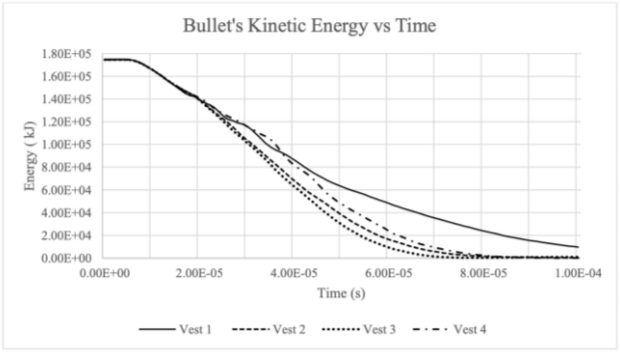

Figure 15. Comparison of Bullet's Kinetic Energy for All Vests

 https://doi.org/ 10.25077/metal.9.1.1-13.2025

3.8. Overall Comparison

- Vest 1 (Solid Line): Kinetic energy reduction is stable but remains high, indicating that the bullet is not completely stopped, resulting in partial penetration—low stopping power due to its basic material and layer structure.
- Vest 2 (Dashed Line): Demonstrates better energy reduction than Vest 1, with minimal residual energy. The layered structure of Vest 2 offers more effective protection, although it is less efficient than Vest 3 in absorbing kinetic energy.
- Vest 3 (Dotted Line): This vest is the most effective in absorbing energy among others. The sandwich design (Titanium-PVC-UHMWPE) facilitates more efficient energy absorption, effectively stopping the bullet.
- Vest 4 (Dash-Dot Line): Superior to Vest 1 but slower in stopping the bullet compared to Vest 2 and Vest 3. The gradual energy kinetic reduction gives more protection to the wearer. More importantly, there is no indication of spalling phenomenon which has a risk for the wearer.

4. DISCUSSIONS

The results from both the experimental tests and numerical simulations provided valuable insights into the performance of the different vest configurations. Vest 1, which had fewer UHMWPE layers along with a single titanium sheet and PVC layers, offered moderate protection but struggled under high-velocity impacts. While the BFS values remained within the NIJ standard limit of 44 mm, they were relatively high (ranging from 31.13 mm to 38.03 mm), indicating a higher risk of blunt trauma. Additionally, in multiple tests, the vest was fully penetrated, highlighting its limited energy absorption capacity.

Vest 2, with its sandwich-layered design, significantly outperformed Vest 1. By incorporating additional UHMWPE layers and a second titanium plate, it effectively reduced BFS values to a much safer range (9.88 mm to 16.36 mm). This confirmed that a multi-layered approach improves energy dissipation and impact resistance. The numerical simulations closely aligned with experimental results, reinforcing the reliability of the finite element model used in this study.

Building on these findings, two additional vest designs—Vest 3 and Vest 4—were proposed to further enhance ballistic protection. Vest 3 features a sandwich structure with 20 layers of UHMWPE, PVC layers, and titanium plates on both the front and back, offering a reinforced design for maximum impact absorption. Numerical simulations showed that Vest 3 delivered the best performance in stopping the bullet in the shortest distance and demonstrating the most effective energy dissipation.

Vest 4, designed with a double titanium front face and an internal PVC layer, aimed to balance protection and wearer safety. It performed better than Vest 2 but slightly lagged behind Vest 3 in terms of energy absorption and stopping power. On the other hand, the gradual energy dissipation of Vest 4 provided better protection against blunt force trauma.

Overall, Vest 3 demonstrated the best ballistic performance among all configurations**,** achieving the most efficient energy absorption and bullet-stopping capability. However, the spalling phenomenon must be addressed to ensure wearer safety. Future research should focus on refining material combinations and optimizing the layering sequence to mitigate this issue. Additionally, experimental validation of Vest 3 and Vest 4 is necessary to confirm their real-world effectiveness.

Moving forward, optimizing vest configurations, exploring alternative materials, and testing against higher-caliber projectiles could lead to the development of next-generation bulletproof vests that provide superior protection without compromising comfort and mobility.

5. CONCLUSION

The results from both the experimental tests and numerical simulations provided valuable insights

into the performance of the different vest configurations. Vest 1, which had fewer UHMWPE layers along with a single titanium sheet and PVC layers, offered moderate protection but struggled under high-velocity impacts. While the BFS values remained within the NIJ standard limit of 44 mm, they were relatively high (ranging from 31.13 mm to 38.03 mm), indicating a higher risk of blunt trauma. Additionally, in multiple tests, the vest was fully penetrated, highlighting its limited energy absorption capacity.

Vest 2, with its sandwich-layered design, significantly outperformed Vest 1. By incorporating additional UHMWPE layers and a second titanium plate, it effectively reduced BFS values to a much safer range (9.88 mm to 16.36 mm). This confirmed that a multi-layered approach improves energy dissipation and impact resistance. The numerical simulations closely aligned with experimental results, reinforcing the reliability of the finite element model used in this study.

Building on these findings, two additional vest designs—Vest 3 and Vest 4—were proposed to further enhance ballistic protection. Vest 3 features a sandwich structure with 20 layers of UHMWPE, PVC layers, and titanium plates on both the front and back, offering a reinforced design for maximum impact absorption. Numerical simulations showed that Vest 3 delivered the best performance in stopping the bullet in the shortest distance and demonstrating the most effective energy dissipation.

Vest 4, designed with a double titanium front face and an internal PVC layer, aimed to balance protection and wearer safety. It performed better than Vest 2 but slightly lagged behind Vest 3 in terms of energy absorption and stopping power. On the other hand, the gradual energy dissipation of Vest 4 provided better protection against blunt force trauma.

Overall, Vest 3 demonstrated the best ballistic performance among all configurations, achieving the most efficient energy absorption and bullet-stopping capability. However, the spalling phenomenon must be addressed to ensure wearer safety. Future research should focus on refining material combinations and optimizing the layering sequence to mitigate this issue. Additionally, experimental validation of Vest 3 and Vest 4 is necessary to confirm their real-world effectiveness.

Moving forward, optimizing vest configurations, exploring alternative materials, and testing against higher-caliber projectiles could lead to the development of next-generation bulletproof vests that provide superior protection without compromising comfort and mobility.

REFERENCES

[1] P. J. Hazell, Armour: Materials, Theory, and Design (2nd ed.), 2nd ed. Boca Raton: CRC Press, 2022.

[2] M. A. Abtew, F. Boussu, and P. Bruniaux, “Dynamic impact protective body armour: A comprehensive appraisal on panel engineering design and its prospective materials,” Def. Technol., vol. 17, no. 6, pp. 2027–2049, 2021, doi: 10.1016/j.dt.2021.03.016.

[3] J. Lin, Y. Li, S. Liu, and H. Fan, “Numerical investigation of the high-velocity impact performance of body armor panels,” Thin-Walled Struct., vol. 189, no. June, p. 110909, 2023, doi: 10.1016/j.tws.2023.110909.

[4] J. Rice, “An investigation into the viablility of ceramic foam and ultra high molecular weight polyethylene composite for ballistic arrest,” 2021.

[5] W. J. Stronge, “Impact Mechanics: Second Edition,” in Impact Mechanics, Second Edition, 2nd ed., Cambridge University Press, 2018, pp. 1–27.

[6] N. Zhou, J. Zhu, J. Jiang, and G. Zhou, “Experimental investigation on ballistics resistance of UHMWPE fiber laminates,” J. Phys. Conf. Ser., vol. 2285, no. 1, 2022, doi: 10.1088/1742-6596/2285/1/012032.

[7] L. Chen, M. Cao, and Q. Fang, “Ballistic performance of ultra-high molecular weight polyethylene laminate with different thickness,” Int. J. Impact Eng., vol. 156, p. 103931, 2021, doi: 10.1016/j.ijimpeng.2021.103931.

[8] L. Ding, X. Gu, P. Shen, and X. Kong, “Ballistic Limit of UHMWPE Composite Armor under Impact of Ogive-Nose Projectile,” Polymers (Basel)., vol. 14, no. 22, pp. 0–22, 2022, doi: 10.3390/polym14224866.

[9] H. Mahfuz, M. R. Khan, T. Leventouri, and E. Liarokapis, "Investigation of MWCNT reinforcement on the strain hardening behavior of ultrahigh molecular weight polyethylene," J. Nanotechnol., vol. 2011, 2011, doi: 10.1155/2011/637395.

[10] I. Goda and J. Girardot, "Numerical modeling and analysis of the ballistic impact response of ceramic/composite targets and the influence of cohesive material parameters," Int. J. Damage Mech., vol. 30, no. 7, pp. 1079–1122, 2021, doi: 10.1177/1056789521992107.

[11] L. Gilson et al., "Ballistic impact response of an alumina-based granular material: Experimental and numerical analyses," Powder Technol., vol. 385, pp. 273–286, 2021, doi: 10.1016/j.powtec.2021.02.065.

[12] A. Hassouna, S. Mezlini, and T. Ameur, "Numerical study of ballistic impact of hard bulletproof vests: Effect of the multilayered armors design," Polym. Compos., vol. 44, Sep. 2023, doi: 10.1002/pc.27715.

[13] L. Alves and P. A. F. Martins, "Understanding Invert Forming of Thin-Walled Polyvinyl Chloride Tubes Using a Die Based on a Mechanical Flow Formulation," Mater. Manuf. Process., vol. 24, pp. 1398–1404, Dec. 2009, doi: 10.1080/10426910902997530.

[14] M. A. Nael, D. A. Dikin, N. Admassu, O. B. Elfishi, and S. Percec, "Multilayers Subjected to Concentrated Drop-Weight Impact," pp. 1–15, 2024.

[15] K. M. Higgins, C. K. Lord, S. L. Lightsey, K. Malley, and N. E. Waters, "NIJ Standard–0101.04, Revision A," vol. JR000228, p. 52, 2001, [Online]. Available: https://www.nij.gov/topics/corrections/recidivism/Pages/welcome.aspx.

[16] S. Yaneva, "Ballistic resistance of bulletproof vests level IIIA. Development of testing methodology," MATEC Web Conf., vol. 317, p. 06003, 2020, doi: 10.1051/matecconf/202031706003.

[17] T. Wantang, M. Pipathattakul, and F. Wiwatwongwana, "Sustainable innovation in ballistic vest design: Exploration of polyurethane-coated hemp fabrics and reinforced sandwich epoxy composites against 9 mm and. 40 S&W bullets," J. Met. Mater. Miner., vol. 33, no. 4, pp. 1–11, 2023, doi: 10.55713/JMMM.V33I4.1830.

[18] A. Purushothaman, G. Coimbatore, and S. S. Ramkumar, "Soft body armor for law enforcement applications," J. Eng. Fiber. Fabr., vol. 8, no. 2, pp. 97–103, 2013, doi: 10.1177/155892501300800212.

[19] J. Hong, J. Lim, and W. W. Chen, "Perpendicular Yarn Pull-out Behavior under Dynamic Loading BT - Dynamic Behavior of Materials, Volume 1," 2011, pp. 211–212.

[20] R. Sun, Y. Feng, B. Wang, C. Liu, and C. Shen, "Enhanced interfacial and mechanical property of biodegradable poly(butylene succinate) film via introducing ultrahigh molecular weight polyethylene shish-kebab fibers," Mater. Res. Express, vol. 6, Dec. 2019, doi: 10.1088/2053-1591/ab5ec9.

[21] Livermore Software Technology Corporation, LS-DYNA Keyword User's Manual Volume II R7.1, vol. II, no. 5442. 2014.

[22] M. Ashby, "Material Property Data," Mater. Sustain. Dev., no. October, pp. 461–484, 2024, doi: 10.1016/b978-0-323-98361-7.15001-8.

[23] L. Yan et al., "Dynamic constitutive models of Ti-6Al-4V based on isothermal ture stress–strain curves," J. Mater. Res. Technol., vol. 19, pp. 4733–4744, 2022, doi: https://doi.org/10.1016/j.jmrt.2022.06.164.

[24] A. Sastranegara, K. E. Putra, E. Halawa, N. A. Sutisna, and A. Topa, "Finite Element Analysis on ballistic impact performance of multi-layered bulletproof vest impacted by 9 mm bullet," Sinergi (Indonesia), vol. 27, no. 1, pp. 15–22, 2023, doi: 10.22441/sinergi.2023.1.003.

[25] A. Sastranegara and P. Gautama, "Finite Element Analysis of Ball Bearing Shield Defect Mechanism," J. Tek. Mesin Sinergi, vol. 21, no. 2, pp. 308–319, 2023, doi: 10.31963/sinergi.v21i2.4500.